Rigid conformal polishing tool using non-linear visco-elastic effect

Dae Wook Kim[1]* and James H. Burge[1]

[1]*College of Optical Sciences, University of Arizona, 1630 E. University Blvd, Tucson, Arizona 85721, U.S.A.*
**letter2dwk@hotmail.com*

Abstract: Computer controlled optical surfacing (CCOS) relies on a stable and predictable tool influence function (TIF), which is the shape of the wear function created by the machine. For a polishing lap, which is stroked on the surface, both the TIF stability and surface finish rely on the polishing interface maintaining intimate contact with the workpiece. Pitch tools serve this function for surfaces that are near spherical, where the curvature has small variation across the part. The rigidity of such tools provides natural smoothing of the surface, but limits the application for aspheric surfaces. Highly flexible tools, such as those created with an air bonnet or magnetorheological fluid, conform to the surface, but lack intrinsic stiffness, so they provide little natural smoothing. We present a rigid conformal polishing tool that uses a non-linear visco-elastic medium (*i.e.* non-Newtonian fluid) that conforms to the aspheric shape, yet maintains stability to provide natural smoothing. The analysis, design, and performance of such a polishing tool is presented, showing TIF stability of <10% and providing surface finish with <10Å roughness.

OCIS codes: (220.0220) Optics design and fabrication; (220.4610) Optics fabrication; (220.5450) Polishing.

References and links

1. R. A. Jones, "Computer control for grinding and polishing," Photon. Spectra •••, 34–39 (1963).
2. R. E. Wagner, and R. R. Shannon, "Fabrication of aspherics using a mathematical model for material removal," Appl. Opt. **13**(7), 1683–1689 (1974).
3. R. A. Jones, "Computer-controlled polishing of telescope mirror segments," Opt. Eng. **22**, 236–240 (1983).
4. D. D. Walker, D. Brooks, A. King, R. Freeman, R. Morton, G. McCavana, and S. W. Kim, "The 'Precessions' tooling for polishing and figuring flat, spherical and aspheric surfaces," Opt. Express **11**(8), 958–964 (2003).
5. H. M. Pollicove, E. M. Fess, and J. M. Schoen, "Deterministic manufacturing processes for precision optical surfaces," in *Window and Dome Technologies VIII*, R. W. Tustison, eds., Proc. SPIE **5078**, 90–96 (2003).
6. J. H. Burge, S. Benjamin, D. Caywood, C. Noble, M. Novak, C. Oh, R. Parks, B. Smith, P. Su, M. Valente, and C. Zhao, "Fabrication and testing of 1.4-m convex off-axis aspheric optical surfaces," in *Optical Manufacturing and Testing VIII*, J. H. Burge; O. W. Fähnle and R. Williamson, eds., Proc. SPIE **7426**, 74260L1–12 (2009).
7. C. L. Carnal, C. M. Egert, and K. W. Hylton, "Advanced matrix-based algorithms for ion beam milling of optical components," in *Current Developments in Optical Design and Optical Engineering II*, R. E. Fischer and W. J. Smith, eds., Proc. SPIE **1752**, 54–62 (1992).
8. H. Lee, and M. Yang, "Dwell time algorithm for computer-controlled polishing of small axis-symmetrical aspherical lens mold," Opt. Eng. **40**(9), 1936–1943 (2001).
9. D. W. Kim, S. W. Kim, and J. H. Burge, "Non-sequential optimization technique for a computer controlled optical surfacing process using multiple tool influence functions," Opt. Express **17**(24), 21850–21866 (2009).
10. M. T. Tuell, "Novel tooling for production of aspheric surfaces," M.S. Thesis (2002).
11. R. P. Chhabra, and J. F. Richardson, *Non-Newtonian Flow and Applied Rheology (2nd edition)* (Elsevier Ltd, 2008), Chap. 1.
12. B. C. Don Loomis, Crawford, Norm Schenck, and Bill Anderson, Optical Engineering and Fabrication Facility, University of Arizona, 1630 E. University Blvd, Tucson, Arizona 85721, (personal communication, 2009).
13. M. A. Meyers, and K. K. Chawla, *Mechanical Behavior of Materials (2nd edition)* (Cambridge University Press, 2009), 124–125.
14. A. C. Fischer-Cripps, "Multiple-frequency dynamic nanoindentation testing," J. Mater. Res. **19**(10), 2981–2988 (2004).
15. M. Johns, "The Giant Magellan Telescope (GMT)," in *Extremely Large Telescopes: Which Wavelengths?* T. E. Andersen, eds., Proc. SPIE **6986**, 698603 1–12 (2008).

#119551 - $15.00 USD Received 5 Nov 2009; revised 27 Dec 2009; accepted 6 Jan 2010; published 20 Jan 2010

16. H. M. Martin, D. S. Anderson, J. R. P. Angel, R. H. Nagel, S. C. West, and R. S. Young, "Progress in the stressed-lap polishing of a 1.8-m f/1 mirror," in *Advanced Technology Optical Telescopes IV*, L. D. Barr, eds., Proc. SPIE **1236**, 682–690 (1990).
17. D. W. Kim, W. H. Park, S. W. Kim, and J. H. Burge, "Parametric modeling of edge effects for polishing tool influence functions," Opt. Express **17**(7), 5656–5665 (2009).
18. D. W. Kim, W. H. Park, S. W. Kim, and J. H. Burge, "Edge tool influence function library using the parametric edge model for computer controlled optical surfacing," in *Optical Manufacturing and Testing VIII*, J. H. Burge; O. W. Fähnle and R. Williamson, Proc. SPIE **7426**, 74260G1–12 (2009).
19. R. E. Parks, "Alignment of off-axis conic mirrors," in *Optical Fabrication and Testing*, OSA Technical Digest Series (Optical Society of America, 1980), paper TuB4.
20. Bellofram Corporation, "Bellofram rolling diaphragm design manual" (2009), *http://www.atcdiversified.com/Diaphragm/PDF/design_manual.pdf*.
21. S. Benjamin, Optical Engineering and Fabrication Facility, University of Arizona, 1630 E. University Blvd, Tucson, Arizona 85721, (personal communication, 2009).
22. J. H. Burge, College of Optical Sciences, University of Arizona, 1630 East University Boulevard, Tucson, AZ 85721, is preparing a manuscript to be called "High speed polishing lap for efficient computer controlled optical surfacing."
23. J. Nelson, and G. H. Sanders, "The status of the Thirty Meter Telescope project," in *Ground-based and Airborne Telescopes II*, L. M. Stepp and R. Gilmozzi, eds., Proc. SPIE **7012**, 70121A1–18 (2008).
24. A. Heller, "Safe and sustainable energy with LIFE" (2009), *https://str.llnl.gov/AprMay09/pdfs/05.09.02.pdf*.
25. D. W. Kim, College of Optical Sciences, University of Arizona, 1630 East University Boulevard, Tucson, AZ 85721, and J. H. Burge are preparing a manuscript to be called "Parametric smoothing model for rigid conformal polishing laps that use visco-elastic materials."

1. Introduction

Various computer controlled optical surfacing (CCOS) processes have been developed since the 1960s [1–6]. CCOS processes can provide good solutions for fabrication of precision optics because of their high convergence rate based on deterministic removal processes. Many large aspheric optical surfaces and off-axis segments have been successfully fabricated using these techniques [4–6].

Most CCOS processes are based on three main components, i) a numerically controlled (NC) polishing machine, ii) embedded process control intelligence (*i.e.* process optimization software) and iii) a polishing tool. The NC polishing machine provides a stable and repeatable control environment to move the polishing tool on a workpiece. The embedded process control intelligence designs polishing run parameters, such as tool RPM(revolutions per minute), tool pressure, and dwell time map (*i.e.* tool ablation time as a function of tool position on a workpiece) to achieve a target removal map. For an optimal polishing run, there have been many studies about optimization techniques used in embedded intelligence [7–9]. The last component, the polishing tool, makes the actual contact and removes material from the workpiece.

In general, a dwell time map is the main optimization result from the process control intelligence to achieve a given target removal map. This optimization is mainly based on a de-convolution process of the target removal map using a tool influence function (TIF). The TIF is the instantaneous material removal under the polishing tool for a given tool motion. Then, the control intelligence uses the TIF as a building block to achieve the target removal map by spatially distributing and accumulating the TIF blocks on the workpiece. Thus, having a stable and deterministic TIF is a critical element for a successful CCOS process.

The TIF is a direct function of tool properties, such as pressure distribution under the tool, tool contact area shape, tool motion, and so forth. Thus, developing a well-behaved tool is an essential component to achieve a deterministic TIF. Tool development for aspheric (or freeform) optics production is an especially complex problem. Because local curvatures of an aspheric surface vary as a function of position on a workpiece, a tool with a rigid surface shape cannot be used. Instead, flexibility is required to maintain good contact with the workpiece surface, and not leave zones in the workpiece surface figure due to the tool-workpiece misfit. However, the smoothing effect that automatically compensates for high spatial frequency errors on the workpiece by a rigid tool hitting high portions with higher pressure on a rough surface disappears as a tool becomes too compliant [10]. Thus, tool development is the art of balancing between flexibility and rigidity.

#119551 - $15.00 USD Received 5 Nov 2009; revised 27 Dec 2009; accepted 6 Jan 2010; published 20 Jan 2010

There are three general types of polishing tools, i) rigid tools, ii) semi-flexible tools, and iii) compliant tools. Each type has its own optimal flexibility and rigidity for its major purpose as a polishing tool. (A general comparison between different tool types is given in Section 2.3.) However, it is very difficult to balance between flexibility and rigidity due to their conflicting characteristics.

The present work introduces a rigid conformal (RC) tool, which uses a non-Newtonian fluid (*a.k.a.* solid-liquid) that has both flexibility and rigidity for different time scales. (*Note*: A US provisional patent was filed for the RC lap.) Section 2 provides a theoretical background including a brief introduction about the properties of the non-Newtonian fluid. An actual RC lap along with its schematic structural design is presented in Section 3. Some experimental performance demonstrations of the RC lap are given in Section 4.

2. Theoretical background

2.1 Non-Newtonian fluid

Since the days of Sir Isaac Newton, opticians have relied on the visco-elastic properties of pitch to create effective polishing tools. Pitch acts as a highly viscous Newtonian fluid for long time scales – it undergoes shear motion that is proportional to the shear stress, so it flows to conform to the shape of the workpiece. At constant temperature, this flow is characterized by the viscosity and is described by the Navier-Stokes equations [11]. Pitch has two principal limitations for polishing: the TIF tends to be unstable, and it does not flow fast enough to accommodate the use of large tools on steep aspheric surfaces [12].

In order to insure that the tool conforms to the surface, we desire a lap made from a material that will flow much more quickly than pitch. Yet we wish to maintain the tool's rigid behavior to preserve the natural smoothing abilities. Such a tool can be made by replacing the pitch with a visco-elastic non-Newtonian fluid. The visco-elastic fluid will act like a solid for a short time period under stress. If stress is applied over a long time period, it flows like a liquid.

A bar made of non-Newtonian silastic polymer (SP) (~2 × 2 × 15cm pink bar) was hand-molded as shown in Fig. 1.

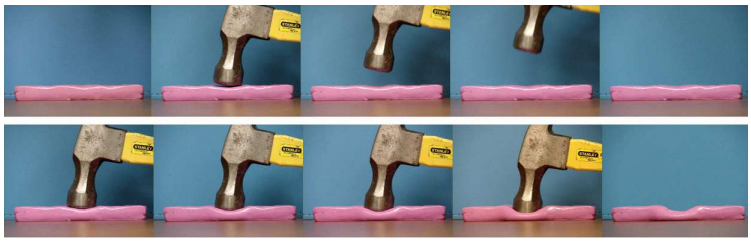

Fig. 1. Two phases of a visco-elastic non-Newtonian silastic polymer: solid-like phase for <~0.1 seconds hammering impulse (top), and liquid-like phase for ~17 seconds long stress by hammer's weight (bottom), (Note: These pictures are edited to contrast the two phases. A more comprehensive view is provided in the accompanying movie clip, Media 1.)

In the upper figure, the bar was hammered for less than ~0.1 seconds. The bar was deformed by a small amount after the harsh impact. This is the solid-like behavior of the non-Newtonian fluid. The lower figure shows a large deformation of the bar. When the hammer was gently placed on the bar loaded by only its weight, the bar started to flow just like a liquid. The duration of the load was ~17 seconds, much longer than the hammer strike case. The accompanying movie clip (Media 1) clearly contrasts these two opposite phases. (The time duration threshold that distinguishes the two phases varies for different non-Newtonian fluids.)

2.2 Dynamic modulus and smoothing effect of non-Newtonian fluid

Non-Newtonian fluids can resist deformation in a solid-like or fluid-like (*i.e.* viscous) manner depending on the applied frequencies of stress. In order to quantitatively understand these

#119551 - $15.00 USD Received 5 Nov 2009; revised 27 Dec 2009; accepted 6 Jan 2010; published 20 Jan 2010

characteristics, the dynamic modulus is used. The dynamic modulus is defined as the ratio of the stress to strain under an oscillating stress condition. These oscillating strain and stress relationships can be expressed as

$$\varepsilon = \varepsilon_0 \sin(t\omega) \tag{1}$$

$$\sigma = \sigma_0 \sin(t\omega + \delta) \tag{2}$$

where ε is time dependent strain, ε_0 is magnitude of the strain, t is time, ω is angular frequency of oscillation, σ is time dependent stress, σ_0 is magnitude of the stress, and δ is phase lag between the stress and strain.

For an ideal solid, the strain and stress are oscillating in phase (*i.e.* $\delta = 0°$). If the material is an ideal viscous fluid, the stress is 90° out of phase (*i.e.* $\delta = 90°$) with the strain.

For these oscillating stress and strain, the tensile storage modulus and loss modulus are defined to quantify the solid-like and fluid-like properties as below [13].

$$Storage\ modulus : E' = \frac{\sigma_0}{\varepsilon_0}\cos\delta \tag{3}$$

$$Loss\ modulus : E'' = \frac{\sigma_0}{\varepsilon_0}\sin\delta \tag{4}$$

The storage modulus is related to the elastic deformation, and the loss modulus is related to the time-dependent viscous behavior of a non-Newtonian fluid.

A loss tangent, the ratio between the storage and loss modulus, is a convenient measure of the relative contribution of the solid-like to fluid-like mechanical responses [13]. The loss tangent is defined as

$$\tan\delta = \frac{E''}{E'} \tag{5}$$

where $\tan\delta$ is the loss factor. For instance, $\tan\delta > 1$ indicates a fluid-like behavior of the material. If $\tan\delta < 1$, it means that the solid-like response is predominant over the fluid-like response.

Some measured storage modulus and loss tangent values for fused silica and Silly-Putty™ (Silly-Putty is a trademark of Crayola LLC.) were obtained from the literature, and are shown in Fig. 2 [14]. Fused silica can be regarded as an elastic solid, so that the loss tangent is almost zero. Also, the storage modulus is almost a constant ~70GPa over the 0-10Hz frequency range of the oscillating stress. In contrast, the Silly-Putty™ is a non-Newtonian fluid, which has an inorganic polymer with visco-elastic agent (polydimethylsiloxane) in it. The frequency-dependent behavior is clearly shown in Fig. 2 (right). Based on the loss tangent values, Silly-Putty™ begins to act like a solid when the applied stress is oscillating at more than ~1Hz [14]. Also, the storage modulus E' in the high frequency range (*i.e.* >5Hz) is ~30 times larger than the low frequency range (*i.e.* <0.2Hz) values.

#119551 - $15.00 USD Received 5 Nov 2009; revised 27 Dec 2009; accepted 6 Jan 2010; published 20 Jan 2010

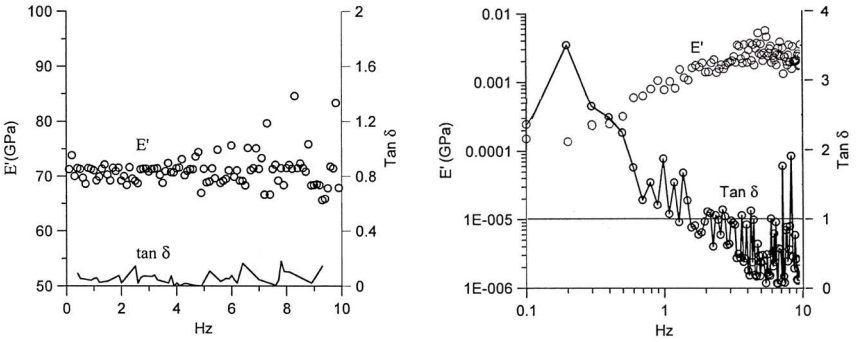

Fig. 2. Storage modulus E' and loss factor $tan\delta$ for fused silica (left) and Silly-Putty™ (right) as a function of applied stress frequency from the literature [14]

The storage modulus plays an important role in estimating the smoothing effect of a tool. The storage modulus defines how much local pressure is required for a tool to be deformed by a local bump on the workpiece as shown in Fig. 3. If an elastic material has a thickness L and storage modulus E', the additional local pressure (on top of the nominal polishing pressure) due to ΔL bump deformation can be calculated from Eq. (3) as

$$P_{add} = \sigma_0 = \varepsilon_0 \cdot \frac{E'}{\cos\delta} = \frac{\Delta L}{L} \cdot \frac{E'}{\cos\delta} \tag{6}$$

where P_{add} is the additional local pressure.

If the deformed local area is small enough compared to the whole tool area, the change in the nominal pressure due to the induced local pressure may be ignored. Then, this additional local pressure can be added to the nominal polishing pressure. The higher local polishing pressure on the bump is

$$P_{bump} = P_{nominal} + P_{add} \tag{7}$$

where $P_{nominal}$ is the nominal polishing pressure without the bump.

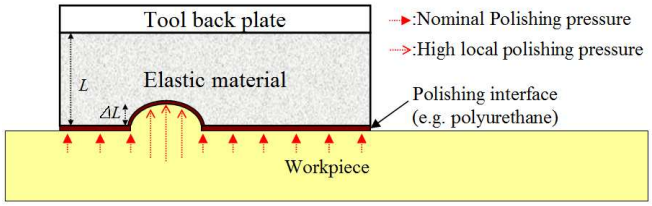

Fig. 3. Locally deformed elastic material due to a bump

For instance, if a tool using L = 1cm thick elastic material with 0.003GPa storage modulus material (*e.g.* Silly-Putty™ with ~10Hz tool motion relative to the surface features) meets a ΔL = 1μm bump, and is locally deformed by it, then the additional local pressure on the bump is 0.043psi using Eq. (6). (The phase lag δ is assumed as 0, because the loss tangent was ~0 at around 10Hz.) Thus, if the nominal pressure under the tool is 0.4psi, the bump feels an additional ~0.04psi, which results in increased removal, which wears down the bump.

2.3 Comparison between RC lap and other tools

As briefly mentioned in Section 1 there are three general types of polishing tools: i) rigid tools, ii) semi-flexible tools, iii) compliant tools. The schematic structures for different tool types are depicted in Fig. 4. Some general advantages and disadvantages of each type are summarized in Table 1. However, we duly acknowledge that the actual characteristics for a specific tool may not agree with this generalized comparison.

#119551 - $15.00 USD Received 5 Nov 2009; revised 27 Dec 2009; accepted 6 Jan 2010; published 20 Jan 2010

The most conventional and common polishing tools are rigid tools (*e.g.* a pitch tool on a thick aluminum back plate). These tools are usually built with a stiff material as a tool base structure. A polishing material, such as pitch or a polyurethane pad is placed under the base plate as a polishing interface. Because the polishing surface shape of the tool is fixed (or changes very slowly) during the polishing run, it needs to be conditioned to fit a workpiece before using it. Otherwise, a misfit may cause radial zones in the workpiece surface figure. It is clear that this type of tool is very good for spherical surface polishing, which has same curvature everywhere on the workpiece. It is relatively easy to make a large tool (*e.g.* 2m diameter tool), and the tool manufacturing cost is usually low. Availability of a large tool is especially important for large optics production (*e.g.* >4m diameter), because the tool size is directly related to the speed of material removal. For instance, the 8.4m Giant Magellan Telescope primary segment [15] cannot be fabricated using a 10cm tool. A 10cm tool would take ~350 hours to polish a 1um thickness of material from the ~55m^2 workpiece area assuming nominal polishing condition values such as 1psi tool pressure, 1m/sec relative speed between the tool and workpiece, and 20um/psi(m/sec)hr Preston constant. Because rigid tools have very small local compliance, they show a good smoothing effect [10,12]. However, these rigid tools need to be customized for each workpiece. Also, the polishing surface of the tool needs to be carefully maintained once it fits to the workpiece. It has, however, an intrinsic limitation in fabricating aspheric (or freeform) workpieces. The rigid tool cannot follow the local curvature (or shape) changes as the tool moves on the workpiece.

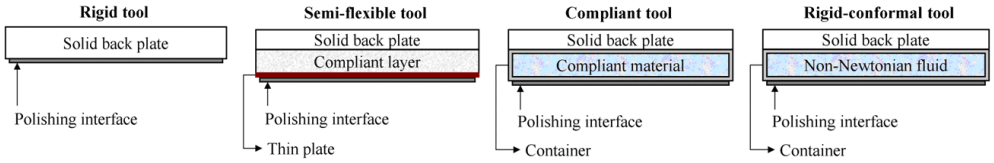

Fig. 4. Schematic tool structures of four different tool types

The semi-flexible tool is carefully designed to fit the varying low order curvature changes while the tool moves on the workpiece. It usually uses a relatively thin metal plate as a tool base, so that the plate's low order bending modes fit the workpiece local curvatures. A foam layer may be placed between the thin plate and another base structure such as thick plate. A polishing pad or pitch is used under the semi-flexible thin plate as a polishing interface. The bending modes can be utilized actively (*e.g.* stress-lap [16] using actuators) or passively (*e.g.* membrane tool [10] using tool's self weight under the gravity). Because these tools try to balance flexibility and rigidity, they can be used for various workpieces including aspheric surfaces. These tools can fit to a workpiece surface, while still providing excellent smoothing effects. Also, a large tool can be manufactured without great difficulty. However, for a passive semi-flexible tool, it must be designed for a specific workpiece by means of a careful and usually time consuming finite element analysis. This design process may be more complicated for the freeform cases than the aspheric cases due to the complex shapes of the freeform surfaces. The actual performance of a new tool needs to be verified and calibrated before use, which is not a trivial task. For an active semi-flexible tool, complex structures to control the bending modes are required. For instance, the stress-lap has many actuators to control the tension on metal wires that are connected to the posts around the perimeter of the circular metal plate [16]. (Because this metal plate is relatively thicker than the thin metal plate in the membrane tool, the stress-lap is often regarded as an actively controlled rigid tool.) By actively pulling or releasing the wires, the metal plate's shape can be controlled. However, the actual bending or pressure distribution under the tool is not easily predicted, so the removal prediction becomes complicated.

The compliant tool can be regarded as the extreme opposite to the rigid tool. This type of tool utilizes compliant materials, such as a liquid or air. Those materials are often sealed in a container (*e.g.* Zeeko's Precessions™ using an inflated membrane polisher [4]) or they make direct contact with the workpiece (*e.g.* QED's MRF™ using a magneto-rheological fluid on a

#119551 - $15.00 USD Received 5 Nov 2009; revised 27 Dec 2009; accepted 6 Jan 2010; published 20 Jan 2010

spinning wheel [5]). These polishing tools can conform to virtually any type of workpiece including aspheric and freeform surfaces. Because the tool always maintains a perfect fit, the material removal (*i.e.* TIF) is very deterministic and stable. However, these tools are usually equipped with complex structures to control liquid or air with high accuracy. Making a large tool (*e.g.* >30cm wide contact spot size) can be a very difficult and expensive task. An expensive high performance NC machine is usually required to control the position and motion of the relatively small tool accurately. Small mis-positioning of the small tool may cause tool marks on the finished workpiece surface, and decrease the process convergence rate. Because the tool will conform to the edge of the workpiece, it cannot go over the edge (*i.e.* overhang) for the edge figuring process. As a result, the edge figuring requires a more delicate technique, such as lifting up the tool for smaller and smaller contact spot sizes as it approaches the edge of the workpiece. It has almost no smoothing effect since it fits to all spatial frequency components of the workpiece surface.

Table 1. General comparison between different tool types [a, b]

	Rigid tool	Semi-flexible Tool	Compliant tool	Rigid conformal tool
Making large tool (*e.g.* >30cm)	Easy	Easy	Difficult	Easy
Cost (including a NC machine)	Inexpensive	Medium	Expensive	Inexpensive
A tool for different workpieces	No	Limited	Yes	Yes
Smoothing	Good	Good	Poor	Medium [25]
Predictability	Low	Fair	Excellent	Good
Fitting to workpiece surface	Poor	Fair	Good	Good
Working on aspheric workpiece	Difficult	Good	Easy	Easy[c]
Working on freeform workpiece	Difficult	Hard	Easy	Easy[c]
Working over the edge	Yes	Yes	No	Yes [17]
Tool maintenance	Difficult	Easy	Medium	Easy

[a]Blue items are usually regarded as advantages.
[b]This is just a general comparison. These characteristics may vary for a specific tool.
[c]These are the expected performance based on the visco-elastic characteristic of the non-Newtonian fluid. They have not been demonstrated yet.

The new RC lap takes the advantages from both the rigid and compliant tool in two different time scales. Also, it is not difficult to make a large RC lap (*e.g.* >30cm diameter tool) because the non-Newtonian fluid is more easily handled (or contained) than a liquid or air. A manufactured 330mm diameter RC lap working on the 8.4m diameter Giant Magellan Telescope (GMT) off axis segment is presented in Section 3.3. The tool manufacturing cost is low.

Because the tool motion (*e.g.* orbital motion in Fig. 5) is usually fast (*e.g.* >10Hz) relative to the local features under the motion (*e.g.* bumps), the RC lap acts like a high storage modulus rigid tool with respect to that time scale as mentioned in Section 2.2. For instance, if the tool is orbiting at 100RPM on a bumpy area on the workpiece, the tool rubs on the bumps with high local pressure. Thus, it can smooth the bumpy surface. Also, the RC lap can go over the edge of the workpiece because the tool does not conform to the edge as long as the tool spins or orbits at high speed. The edge removal characteristic of RC lap was reported in another paper [17,18]. However, the tool still fits to the local curvature changes of the workpiece since the RC lap moves on the workpiece relatively slowly (*e.g.* ~1 RPM workpiece rotation) along the tool path in Fig. 5. (This local curvature characteristic is well described in a literature by Parks [19].) For instance, for an off-axis parabolic workpiece, the tool may travel around the workpiece once a minute while it keep making the high speed orbital motion. (Because of the astigmatic local departure from the best fit sphere of the off-axis workpiece [19], an orbital tool motion will be used to keep the tool's orientation with respect to the workpiece.) The tool will fit to the slowly varying local curvature of the off-axis part as it moves on the workpiece. The non-Newtonian fluid flows like a liquid for this long time scale motion as mentioned in Section 2.2. Thus, a RC lap can be used for aspheric or

#119551 - $15.00 USD Received 5 Nov 2009; revised 27 Dec 2009; accepted 6 Jan 2010; published 20 Jan 2010

freeform surfaces like a compliant tool. This working concept of the RC lap is depicted in Fig. 5.

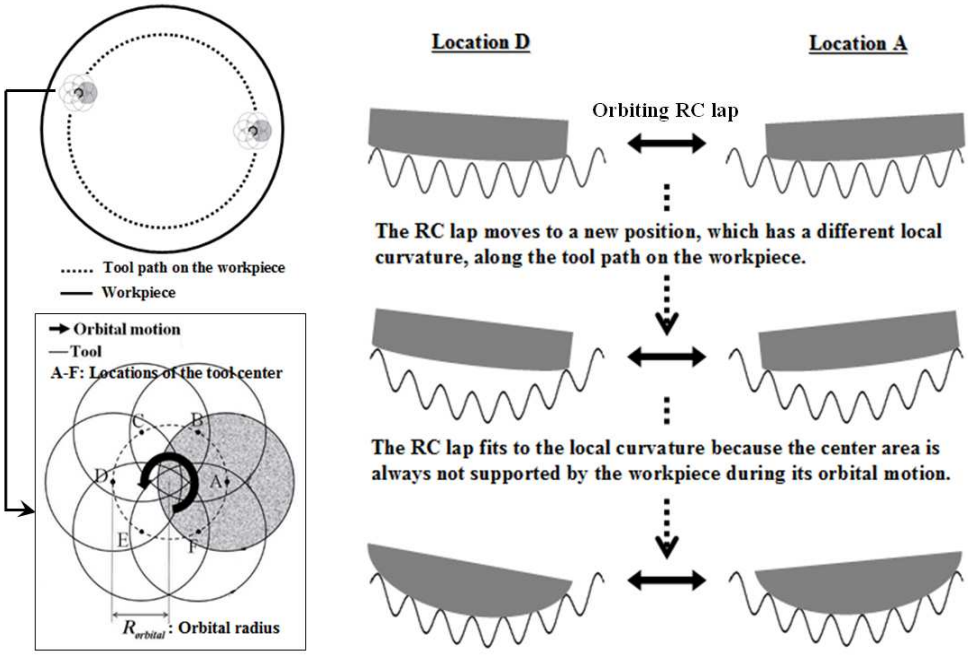

Fig. 5. Working concept of the RC lap with orbital tool motion

However, this working concept needs to be demonstrated with a series of experiments. There may be three main verification steps. The first step is demonstrating the general performance of the RC lap, such as removal rate stability, deterministic TIF, surface finish. The second step is the investigation of smoothing effects to check if the solid-like behavior of the non-Newtonian fluid smoothes out the mid-spatial frequency errors. The final step is the demonstration of the actual flow characteristic of the RC lap.

The major scope of this paper was only the first step, demonstration of the general performance of the RC lap. The smoothing effects of the RC lap are discussed in Section 4.6 briefly. A detailed quantitative smoothing model will be reported in a separate manuscript [25] due to the lengthy discussions in it. We acknowledge that the last topic, flow characteristic of the RC lap, has not been quantitatively studied yet. The premise about the liquid-like behavior of the RC lap will be investigated and demonstrated in future studies.

3. Rigid conformal lap using non-Newtonian fluid

3.1 Schematic RC lap structure

A schematic 3D model for a RC lap is depicted in Fig. 6. It is a polishing tool filled with a non-Newtonian silastic polymer. The silastic polymer is contained between a back plate and a diaphragm. The diaphragm provides a tough and flexible seal to contain the non-Newtonian fluid during polishing runs. It is made out of a layer of woven fabric impregnated with a thin layer of elastomer [20], and the total thickness is between 0.38 and 1.14mm. The polishing pad is placed on the diaphragm. This is the actual contact interface with the workpiece. The polishing pad can be polyurethane, polishing cloth, and so forth. The polishing pad may be tiled in order to create channels for uniform polishing compound distribution under the tool.

#119551 - $15.00 USD Received 5 Nov 2009; revised 27 Dec 2009; accepted 6 Jan 2010; published 20 Jan 2010

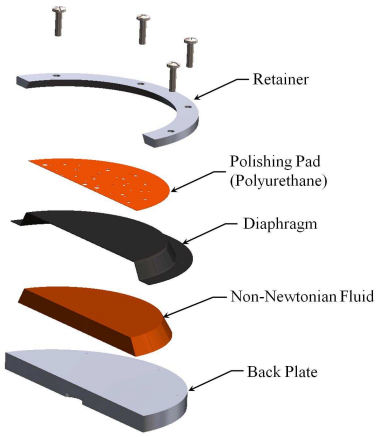

Fig. 6. 3D schematic RC lap structure (exploded and cut in half)

3.2 Forcer design for RC lap

A forcer is usually a drive pin used to provide tool motion as shown in Fig. 7. The interface between the forcer and tool needs to be designed carefully. An over-constrained forcer may apply un-wanted force or moment to a workpiece, which may result in unstable removal due to the disturbed pressure distribution. The workpiece may even be broken. Ideally, the forcer only gives tangential tool motions without any vertical force with respect to the workpiece surface. Polishing pressure comes from the tool's self weight as shown in Fig. 7 (left).

The most common forcer is a drive pin with a ball at the end. The ball goes into the spherical hole on the back plate of a tool as shown in Fig. 7 (middle). By preventing the ball from hitting the bottom of the hole, the forcer does not apply any vertical force to the tool. However, as the drive pin moves, the induced moment from the shear force on the workpiece surface causes a moment and a gradient (*i.e.* linearly varying) polishing pressure distribution. This gradient pressure distribution is shown in Fig. 7 (right).

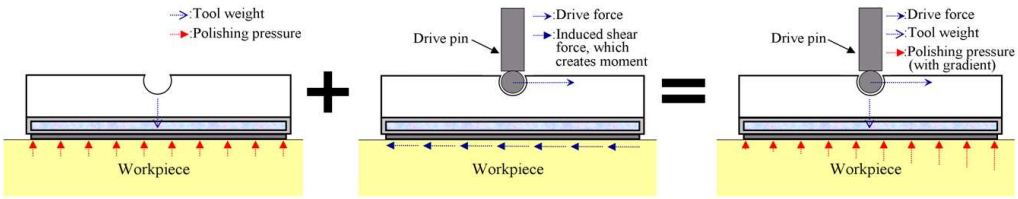

Fig. 7. The gradient net polishing pressure distribution due to the tool weight and the induced moment from the drive force

The forcer for the RC lap was carefully designed to mitigate this unwanted gradient pressure effect. Two different approaches were developed. The first approach was bringing the ball down as closely as possible to the polishing surface, so that the moment from the shear force is minimized. The schematic design is shown in Fig. 8 (left). An actual RC lap with a lowered drive pin hole is shown in Fig. 9 (right). Another approach was a forcer providing a virtual pivot using a number of linkages [21]. The linkages provide a virtual pivot on a workpiece, so that the induced moment becomes zero in theory. This can be very useful for small size tools, which usually have relatively low aspect ratios (*i.e.* thick tools), because they have a steeper pressure gradient. Each end of a linkage is connected to the forcer plate and tool with a ball interface, which allows free rotation in all directions. The schematic configuration for the linkage forcer is presented in Fig. 8 (right).

#119551 - $15.00 USD Received 5 Nov 2009; revised 27 Dec 2009; accepted 6 Jan 2010; published 20 Jan 2010

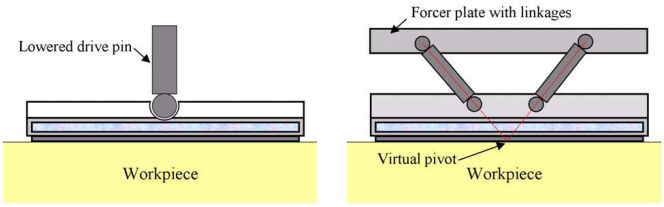

Fig. 8. Schematic forcer designs, which solve the gradient polishing pressure problem in Fig. 7: Lowered drive pin approach (left) and linkage forcer plate approach to provide a virtual pivot (right)

3.3 Manufactured RC lap

Three RC laps (110, 220, and 330mm in diameter) were manufactured. Among many non-Newtonian visco-elastic fluids, Silly Putty™ was used in these RC laps. As shown in Section 2.2, Silly Putty™ has been studied in some other literatures, so that many measured data about its characteristic can be easily acquired. The 220mm RC lap and 330mm RC lap are presented as an example in Fig. 9 and 10, respectively. The 330mm RC lap was used on the 8.4m diameter GMT off axis segment at the Steward Observatory Mirror Lab [15].

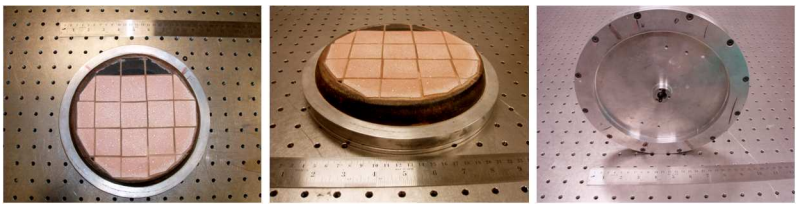

Fig. 9. Manufactured 220mm diameter RC lap (bottom, side, top view from left to right) Three of the polishing pad tiles were intentionally removed to show the structure below. The black seen is the diaphragm shown in Fig. 6.

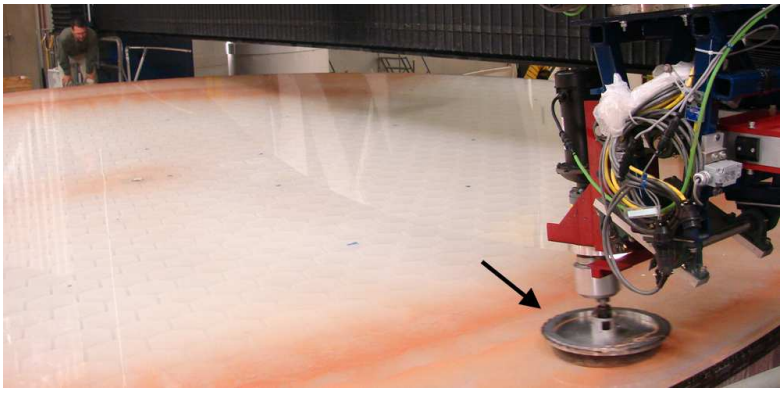

Fig. 10. 330mm diameter RC lap (black arrow) on the 8.4m diameter GMT off axis segment at the Steward Observatory Mirror Lab [15]. (Note: The orbital tool motion is shown in the accompanying movie clip, Media 2.)

A machined aluminum back plate and a Bellofram™ diaphragm [20] were used with a polyurethane polishing pad. A Cerium doped polyurethane polishing pad LP-66 was tiled for channels. (LP-66 is a polyurethane polishing pad sold by Universal Photonics INC.) Detailed specification of the RC laps is listed in Table 2.

#119551 - $15.00 USD Received 5 Nov 2009; revised 27 Dec 2009; accepted 6 Jan 2010; published 20 Jan 2010

Table 2. Specification of three RC laps

Tool diameter	110, 220, 330mm
Aluminum back plate thickness	10mm
Non-Newtonian fluid	Silly-Putty™
Non-Newtonian fluid thickness	10-20mm
Diaphragm	Bellofram™ diaphragm
Polyurethane polishing pad	LP-66 (Cerium doped pad)
Polyurethane polishing pad thickness	0.5mm

4. Performance of rigid conformal lap

4.1 Measured TIF vs. theoretical TIF

One of the most powerful characteristics of the RC lap is highly stable theory-like TIF. The theoretical TIF can be calculated based on the Preston's equation [9]. This stable characteristic mainly comes from the fact that the RC lap always fits to a local workpiece surface and provides a uniform pressure distribution under it. As a result, the TIF does not depend on the shape of the workpiece surface. One of the measured TIFs and a theoretical TIF using the 220mm RC lap with the orbital tool motion are presented as an example in Fig. 11.

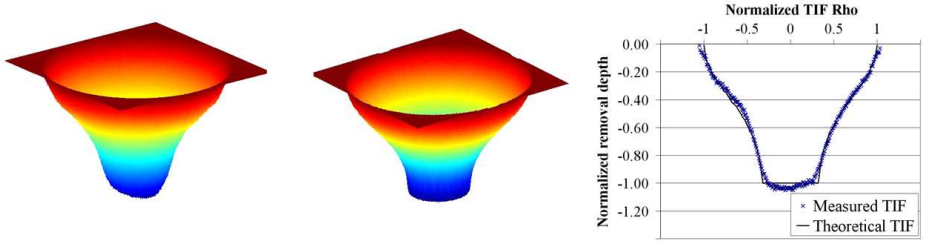

Fig. 11. The TIFs using the RC lap with an orbital tool motion: measured 3D TIF (left), theoretical 3D TIF (middle), and radial profiles of them (right)

The good matching between the measured and theoretical TIFs proves that the removal process can be precisely modeled and predicted using Preston's equation. The deterministic TIFs of the RC lap form good building blocks for the CCOS process. Qualitative results using the measured TIF data are given in Section 4.2-4.4.

4.2 Optimal operation range of RC lap

A series of experiments was conducted to determine the optimal operation range of the RC lap. The optimal operation range was defined as: i) Higher Preston constant (*i.e.* removal rate) is better since it means shorter total polishing time. ii) Preston constant needs to be a constant (or a well characterized function such as a linear function) in the optimal range. iii) Surface roughness after the polishing run needs to be ~2nm RMS. As a reference, a typical pitch tool, which is well known for its superb surface finish, easily gives <1nm RMS surface roughness.

The TIFs were measured as the tool pressure and tool motion speed were varied. A total of 50 experiments were performed, and the removal rates were calculated from the measured TIFs. Also, the surface roughness values were measured for all experiments. Detailed information about the surface roughness measuring device is presented in Section 4.5. The overall experiment conditions are provided in Table 3.

The experiment results are plotted in Fig. 12. Each marker represents the averaged value, and the standard deviation of the value is given as a vertical error bar.

#119551 - $15.00 USD Received 5 Nov 2009; revised 27 Dec 2009; accepted 6 Jan 2010; published 20 Jan 2010

Table 3. Overall TIF experiment conditions

Workpiece	10inch Pyrex
RC lap diameter	110mm
Tool motion	Orbital tool motion
Polishing compound	Rhodite 906 (Cerium based)
Polishing compound particle size	~2μm
Tool pressure range	0.20-0.57psi
Tool motion speed range	0.05-0.22m/sec

For tool pressure variation (0.2-0.57psi), the data showed slightly increasing Preston constant values with increasing pressure as shown in Fig. 12 (left). The surface roughness values in this pressure range were almost constant at ~2nm RMS. Because of the higher Preston constant, we defined 0.3-0.6psi as the optimal operation range of the tool pressure.

The orbital tool motion speed was varied 0.05-0.22m/sec as shown in Fig. 12 (right). A non-linear Preston constant change over the tool speeds range was measured. The Preston constant was stable in the 0.15-0.22m/sec range. The surface roughness was ~2nm RMS for all cases. Thus, 0.15-0.22m/sec was chosen as the optimal tool speed range. However, there is still a good chance to get a stable Preston constant value in even higher speed ranges. This will be evaluated in another investigation [22].

In summary, the optimal RC lap operation range is, i) 0.3-0.6psi for tool pressure, and ii) 0.15-0.22m/sec for tool speed.

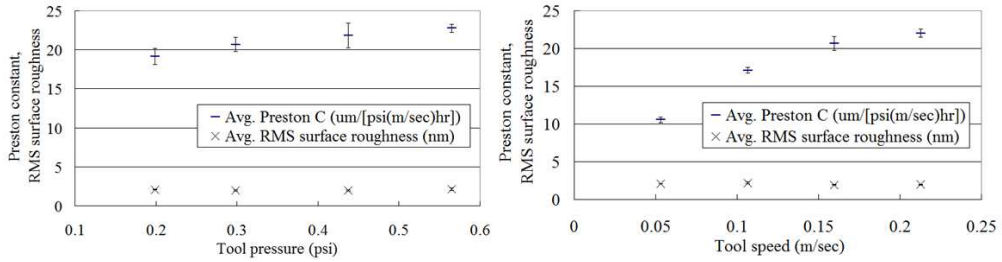

Fig. 12. Preston constant and RMS surface roughness vs. tool pressure (left) or speed (right), (Note: Error-bars represent the standard deviation of the data)

4.3 Dwell time linearity

Most CCOS processes assume that the Preston constant is a fixed value over dwell time. In other words, if a polishing tool stays on a workpiece for twice the time, the material removal from the workpiece should be twice also. This is often called the dwell time linearity.

Two different dwell time values (15 and 30 minutes) were tried for 30 experiments, and the results are presented in Fig. 13.

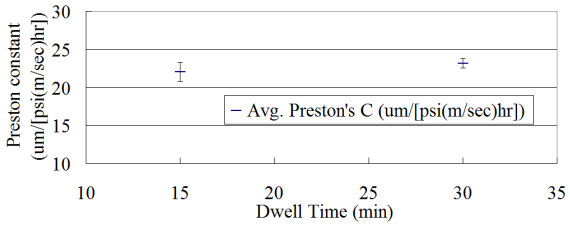

Fig. 13. Preston constant vs. dwell time (Note: Error-bars represent the standard deviation of the data)

The tool was operating within the optimal operation range in Section 4.2. The Preston constant was not changed as we doubled the dwell time. The RC lap shows a good dwell time linearity, which enables a scalable CCOS process.

#119551 - $15.00 USD Received 5 Nov 2009; revised 27 Dec 2009; accepted 6 Jan 2010; published 20 Jan 2010

4.4 Preston constant vs. tool age

A polyurethane polishing pad needs to be conditioned (*i.e.* breaking down the rough pad surface) on a conditioning workpiece (*i.e.* the dummy workpiece) before its first polishing run. In order to qualitatively analyze the conditioning process and the performance of the RC lap after conditioning, the Preston constant and surface roughness values were measured as a function of tool age. The tool age was set to zero when a new polyurethane pad was attached to the RC lap.

Approximately 100 experiments using the 110mm RC lap were conducted on five Pyrex workpieces. The RC lap was run within the optimal RC lap operation range of Section 4.2. The experimental results are plotted in Fig. 14.

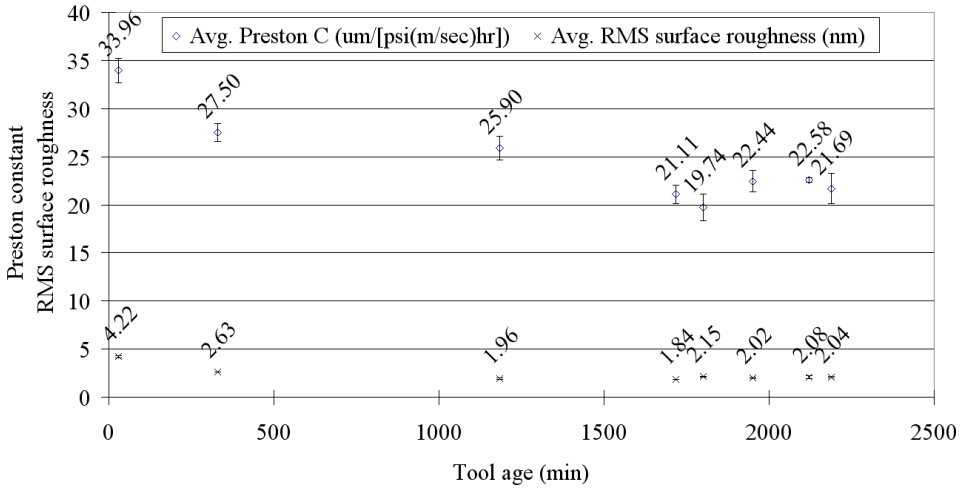

Fig. 14. Preston's constant and RMS surface roughness vs. tool age (Note: Error-bars represent the standard deviation of the value)

The Preston constant values (diamond marker in Fig. 14) were ~34um/[psi(m/sec)hr] when the RC lap was used for the first time. As the tool age approached ~1700minutes, the Preston constant stabilized at ~21um/[psi(m/sec)hr]. The surface roughness values were stable at ~2nm RMS after ~1200minutes tool age. Of course, the tool age axis can be scaled depending on the initial surface roughness of the conditioning workpiece, tool pressure, and tool speed. For instance, higher tool speed and pressure may reduce the conditioning time due to the higher removal per unit time.

Once the RC lap was conditioned (*e.g.* >1700minutes tool age in this case), the Preston constant varied with only ~10% standard deviation. The conditioning process and stable Preston constant after conditioning were successfully demonstrated for the RC lap.

4.5 Surface roughness

The surface roughness after a polishing run is one of the most important criteria used to estimate a tool's performance. If a tool leaves a smooth surface which meets a target specification, the workpiece can be finished using the tool. Otherwise, additional processes using other tools (*e.g.* pitch tools) are required for the final touch-up process to improve the surface roughness [12]. This increases the complexity and time of the CCOS process, so a tool giving a good surface finish is highly desirable.

We reports two experimental results using the RC lap and a pitch tool as shown in Table 4. The surface roughness is a function of many parameters, such as glass material, polishing compound type, and so forth. It is, therefore, invalid to say a tool always gives a certain value for RMS surface roughness. Thus, we acknowledge that there may be a better polishing compound for the pitch tool for this specific set-up, which could have given better

#119551 - $15.00 USD Received 5 Nov 2009; revised 27 Dec 2009; accepted 6 Jan 2010; published 20 Jan 2010

surface finish (*e.g.* 0.2-0.3nm RMS). We provide the pitch tool results in this study only as a brief comparison purposes.

A ULE substrate was used as a common workpiece. The surface roughness after each run was measured using a Wyko NT9800™ interferometer. (Wyko NT9800™ is a trademark of Veeco.) More information about the surface roughness experiment set-up is provided in Table 4.

Table 4. Two surface roughness experiment set-ups

	110mm RC lap	110mm pitch tool
Polishing Compound	Hastilite ZD	Rhodite 906
Tool Motion	Orbital	Orbital
Workpiece	ULE	ULE
Measurement area	~0.2 by 0.3mm	~0.2 by 0.3mm
Sampling interval	484.11nm	484.11nm

The results from 40 experiments are presented in Fig. 15 and 16. Two example surface roughness profiles measured by the Wyko NT9800™ interferometer are presented in Fig. 15. The pitch tool with Rhodite 906 polishing compound provided ~0.9nm RMS surface finish as shown in Fig. 16. The surface finish from the RC lap with Hastilite ZD polishing compound was superb. For 10 repeated experiments, the average surface roughness was ~0.75nm RMS with ~0.1nm standard deviation.

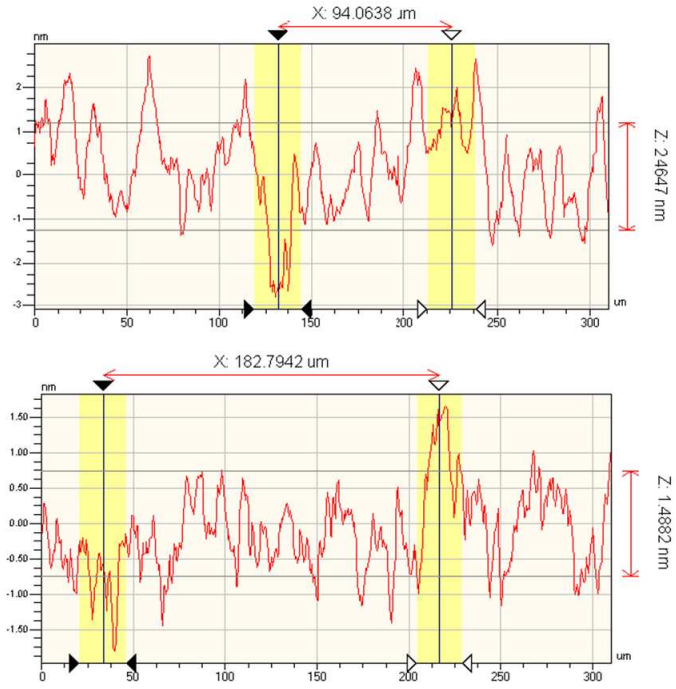

Fig. 15. Two example surface roughness profiles from Wyko NT9800™: pitch tool with Rhodite 906 (top), and RC lap with Hastilite ZD (bottom) (Note: Averaged (in yellow region) peak-to-valley values are provided as additional information.)

#119551 - $15.00 USD Received 5 Nov 2009; revised 27 Dec 2009; accepted 6 Jan 2010; published 20 Jan 2010

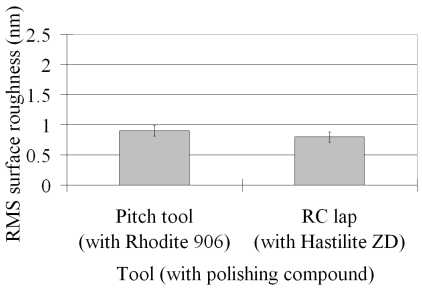

Fig. 16. Surface roughness using a pitch tool and RC lap on a ULE substrate (Note: Error-bars represent the standard deviation of the value)

We have demonstrated that the RC lap, with appropriate polishing compound which depends on a given polishing configuration, can provide a <1nm RMS super smooth surface finish. This may eliminate the need for an extra final touch-up step for most CCOS processes, which usually have <2nm RMS surface roughness target specifications.

4.6 Smoothing effect

A set of smoothing experiments using the 110mm RC lap was performed to verify the smoothing characteristic of the RC lap. A sinusoidal ripple with 12mm period and PV(peak-to-valley) = ~0.4μm was generated on 250mm diameter Pyrex workpieces as shown in Fig. 17 (left). The 12mm ripple period is ~1/10 of the tool diameter, which can be regarded as mid-spatial frequency errors. The initial profile of the ripple is presented in Fig. 17 (right).

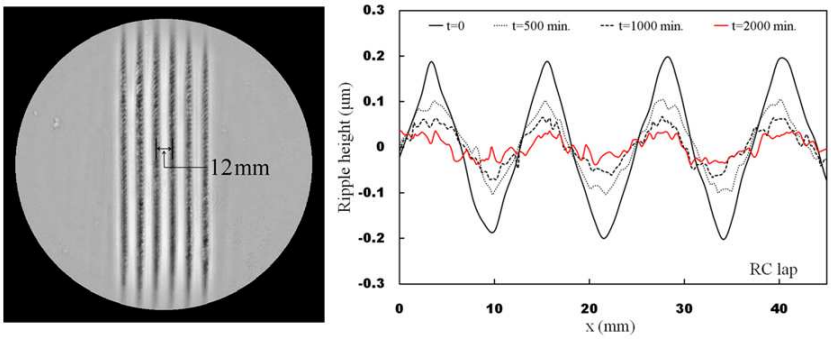

Fig. 17. Grey scale surface map of the Pyrex substrate with sinusoidal ripples (left) and the measured ripple profiles as the RC lap smoothes out the ripples (right).

The RC lap was run with the orbital tool motion on the workpieces until the PV of the ripple was not decreased anymore. Details of the operating condition for the experiments are provided in Table 5.

Table 5. Operating condition for the smoothing experiments using the 110mm RC lap

Workpiece	250mm diameter Pyrex
Tool motion	Orbital tool motion (w/ 30mm orbital radius)
Tool motion speed	94.2mm/sec (*i.e.* 30RPM)
Tool pressure	2500 Pascal (*i.e.* 0.36PSI)
Polishing compound	Rhodite 906 (Cerium based)
Polishing compound particle size	~2μm

The ripples were measured as a function of dwell time of the RC lap on the workpiece using an Intellium™ Fizeau interferometer by ESDI. The measured ripple profiles are shown in Fig. 17 (right), and it is clear that the RC lap smoothed out the mid-spatial frequency errors. After 2000 minutes run, the ripple PV was decreased from ~0.4μm (black solid line) to ~0.077μm (red solid line).

#119551 - $15.00 USD Received 5 Nov 2009; revised 27 Dec 2009; accepted 6 Jan 2010; published 20 Jan 2010

As mentioned in Section 2.2, the storage modulus of a non-Newtonian fluid is a very important clue to understand the smoothing characteristics of the RC lap. However, the actual smoothing process by a tool is entangled with many other factors, such as the actual tool structure including the polishing pad and diaphragm. Also, the fluid dynamics of polishing compounds may play a role in the smoothing process. A quantitative smoothing model using a parametric approach to include those complex factors will be presented as a separate paper with more detailed discussions and experimental data [25] as mentioned in Section 2.3.

5. Concluding remarks

The RC lap exhibits the advantages of rigid and compliant tools in two different time scales using a non-Newtonian fluid. It can be used just like a rigid tool, which has a smoothing effect, with respect to the tool motion (*e.g.* orbital) time scale. As it moves along the tool path on the workpiece, the non-Newtonian fluid is expected to flow to fit the slowly varying local curvatures under the tool. (We acknowledge that this liquid-like characteristic has not been quantitatively demonstrated yet.) The highly deterministic TIF and removal rate was experimentally demonstrated and verified. Also superb surface finish with <1nm RMS surface roughness was achieved on a ULE substrate. In addition to its good performance, the ease with which a large tool can be made in a cost-effective manner makes the RC lap an attractive solution for large precision optics manufacturing CCOS processes. It can also contribute to the realization of some next generation optical systems, which usually have hundreds of aspheric mirrors (*e.g.* Thirty Meter Telescope [23] and Laser Inertial Fusion Engine [24]) or large off axis mirrors (*e.g.* Giant Magellan Telescope [15]).

Acknowledgments

We acknowledge that this work was supported by the Optical Engineering and Fabrication Facility of the College of Optical Sciences at the University of Arizona. We thank Marty Valente (Optical Engineering and Fabrication Facility), Robert Parks (College of Optical Sciences) and Brian Cuerden (Steward Observatory) at the Univ. of Arizona for assistance in the final manuscript preparation. Also, we thank Bill Anderson (Optical Engineering and Fabrication Facility) for performing the experiments and Won Hyun Park (College of Optical Sciences) for providing an idea about the non-Newtonian fluids. The measured data in Fig. 4 was available in this manuscript with the permission of Journal of Materials Research. We thank the journal and A. C. Fischer-Cripps, the author of the original manuscript.

#119551 - $15.00 USD Received 5 Nov 2009; revised 27 Dec 2009; accepted 6 Jan 2010; published 20 Jan 2010